

High-field cyclotron resonance and impurity transition in *n*-type and *p*-type 3C-SiC at magnetic fields up to 175 T

J. Kono,* S. Takeyama,† H. Yokoi,‡ and N. Miura

Institute for Solid State Physics, University of Tokyo, Roppongi, Minato-ku, Tokyo 106, Japan

M. Yamanaka, M. Shinohara, and K. Ikoma

Nissan Research Center, Nissan Motor Co Ltd., Natsushima, Yokosuka, Kanagawa 237, Japan

(Received 3 May 1993)

Magnetotransmission experiments have been carried out on 3C-SiC thin films grown on Si(100) substrates, using the combination of pulsed high magnetic fields up to 175 T generated by the single-turn coil technique and pulsed far-infrared radiations from a H₂O (D₂O) laser at photon energies up to 73.2 meV. In *n*-type 3C-SiC, two cyclotron-resonance (CR) peaks have been observed for $\mathbf{B} \parallel \mathbf{k} \parallel \langle 100 \rangle$ over a wide range of photon energy 10.4–53.8 meV, corresponding to the light- and heavy-mass valleys at the *X* points, i.e., $m_l^* = (0.25 \pm 0.01)m_0$ and $(m_l^* m_h^*)^{1/2} = (0.41 \pm 0.01)m_0$. These values are in agreement with those of Kaplan *et al.* obtained from CR at low fields. This leads to the conclusion that the conduction band in 3C-SiC is very parabolic up to 53.8 meV, and that unlike GaP the effect of camel's-back structure is unobservable. A number of impurity transitions were observed at temperatures below 100 K with photon energies ranging from 34.4 to 73.2 meV. It was found that the observed lines originate from three different donor states which have different binding energies, $E_d = 19, 35, \text{ and } 53 \text{ meV}$. The observation of hole CR was also made in *p*-type 3C-SiC. A broad but prominent peak was observed with an effective mass of $0.45m_0$, at temperatures around 210 K and at a wavelength of 119 μm .

I. INTRODUCTION

Silicon carbide (SiC) has long been of great interest as one of the potential high-temperature semiconductor-device materials which could operate in high-temperature circumstances with high resistance against radiation damage. Because of its high melting point, large band gap, chemical inertness, high hardness, and high thermal conductivity, it has been the prime candidate for such applications, together with semiconducting diamond (C)¹ and boron nitride (BN). Very little is known, however, of its detailed energy-band structure although a considerable amount of research has been undertaken. The main reason for this is the difficulty in growing high-quality single crystals. Its carrier mobility has been very low, and many of the fundamental electronic properties are not yet well enough understood.

Recently, large epitaxial 3C-SiC (Ref. 2) films have been successfully grown on carbonized Si surfaces by the chemical vapor deposition (CVD) technique.^{3,4} Both *n*- and *p*-type specimens have been obtained by introducing active impurities into the crystals.⁴ Very high carrier mobility, up to 3000 cm²/V s at 66 K, for example, have been found in these crystals.⁵

A few experimental works have been so far reported on the band parameters or effective masses of 3C-SiC. All calculations of the energy-band structure of 3C-SiC predict the location of the conduction-band minima to be on the Γ -*X* axis, very close to zone boundary *X*.⁶ The Zeeman luminescence work of Dean, Choyke, and Patrick⁷ confirmed this prediction, and moreover, no evidence was found for a camel's-back structure. The cyclotron-

resonance work of Kaplan *et al.*⁸ yielded both the transverse and longitudinal effective masses of the ellipsoidal energy surface at a photon energy of 3.15 meV: $m_l^* = (0.247 \pm 0.011)m_0$ and $m_h^* = (0.667 \pm 0.015)m_0$. In zinc-blende-type crystals like 3C-SiC, the double degeneracy at the *X* point is lifted into two bands, *X*₁ and *X*₃, due to the lack of inversion symmetry, and the *X*₁-band edge is expected to have a camel's-back structure resulting from the interaction with the *X*₃ band.⁹ If a camel's-back structure exists, the cyclotron mass of m_l^* would have an anomalous energy dependence. This has actually been observed in the conduction band of GaP.¹⁰ Therefore, a high-field cyclotron resonance study of the conduction band at various photon energies can be the best tool for determining whether it has a camel's-back structure or not.

Several works concerning the electron-scattering mechanism in SiC have been reported. Van Daal¹¹ studied the electron mobility in SiC polytypes and found that the temperature dependence of the mobility in 3C-SiC differs significantly from that of 6H- and 15R-SiC, suggesting a different scattering mechanism. Patrick¹² has shown that the high symmetry of 3C-SiC results in very restrictive selection rules for intervalley phonon scattering, which is the dominant mobility-limiting mechanism for other polytypes from 300 to 800 K, and makes the mobility of 3C-SiC higher than that of other polytypes. Study of the cyclotron-resonance linewidth is a powerful tool for investigating the carrier scattering mechanism in semiconductors, and hence should also be very informative for 3C-SiC.

There are considerable disagreements among the

values so far reported for the donor binding energy in *n*-type 3C-SiC.^{4,7,8,13–19} It is well known that undoped CVD-grown 3C-SiC films have residual carriers (electrons). These residual carriers have been considered to be from residual nitrogen donors. However, in recent years, there has been a strong controversy over this origin. From the temperature dependence of carrier density, Suzuki *et al.*¹⁶ deduced that the donors in nondoped samples are not nitrogen but some nonstoichiometric defects. On the other hand, Segall *et al.*,¹⁷ conducting essentially the same experiments, assert that the active donors in all their samples are probably nitrogen. Although nondoped and nitrogen-doped *n*-3C-SiC films have been systematically compared by means of electrical transport,¹⁸ photoluminescence,¹⁹ and electron-spin resonance (ESR),¹⁹ a full understanding of the origin of the residual carriers has not yet been achieved. Far-infrared magneto-optical studies of impurity states have been successfully used in many other semiconductors, but never in 3C-SiC.

The maximum of the valence band is located at $\mathbf{k}=0$ (Γ point) in the Brillouin zone. The wave function at this point is transformed according to the representation Γ_{15} and is triply degenerate (sixfold if spin is included), like III-V compounds with zinc-blende structure. Using the five-level $\mathbf{k}\cdot\mathbf{p}$ analysis of Lawaetz,²⁰ with a modification to include the hole-phonon interaction, Bimberg, Altarelli, and Lipari²¹ calculated the modified Luttinger parameters for the valence band of 3C-SiC to be $\gamma_1^*=2.817$, $\gamma_2^*=0.508$, $\gamma_3^*=0.860$, and $\kappa^*=-0.41$. Large nonparabolicity, resulting from very small spin-orbit splitting (4.5 meV), was predicted for all three valence bands. Available experimental data on the valence-band structure is poor because high-quality *p*-type 3C-SiC has not been achieved.

Recent progress of the megagauss cyclotron-resonance technique has enabled us to investigate energy-band structures in low mobility semiconductors.^{1,22,23} In this paper, we report a detailed investigation of the band structure of 3C-SiC by means of far-infrared cyclotron resonance and impurity transition using pulsed ultrahigh magnetic fields up to 175 T, produced by the single-turn coil technique.²⁴ Section II describes the experimental procedure of the megagauss cyclotron resonance which is common to all the measurements in the present work. Section III is devoted to the description of the experimental results of electron cyclotron resonance. Based on the results, we discuss the location of the conduction-band edge, electron-LO-phonon interaction, and the electron-scattering mechanism. A discussion of impurity transitions is presented in Sec. IV. Finally, a brief description of our observation of hole cyclotron resonance is given in Sec. V.

II. EXPERIMENTAL PROCEDURE

The experimental procedure is essentially the same as the one described in Ref. 1, except for the range of the experimental temperature. The high magnetic fields were pulsed by supplying short large-current pulses of about 2.5 MA to a thin single-turn copper coil from a fast capacitor bank with a storing energy of 100 kJ. Although the coil explodes violently, the movement of fragments is so strongly directed away from the center of the coil that the sample is not destroyed, surviving hundreds of such experiments.

The inner diameter of the single-turn coil was normally 10 mm, which can produce 150 T at maximum. An 8-mm-i.d. (inside diameter) coil was sometimes used, when a higher peak field of 175 T was required. The sample was contained in a small, handmade cryostat which was set at the center of the coil. The temperature of the sample was varied between 10 K and room temperature by controlling the flowing rate of liquid helium in the cryostat. The absolute strength of the magnetic field was determined by measuring the induced voltage in a calibrated pickup coil made of manganese wire wound around the sample. The error of the field measurement

was about 1%. The error of the field measurement

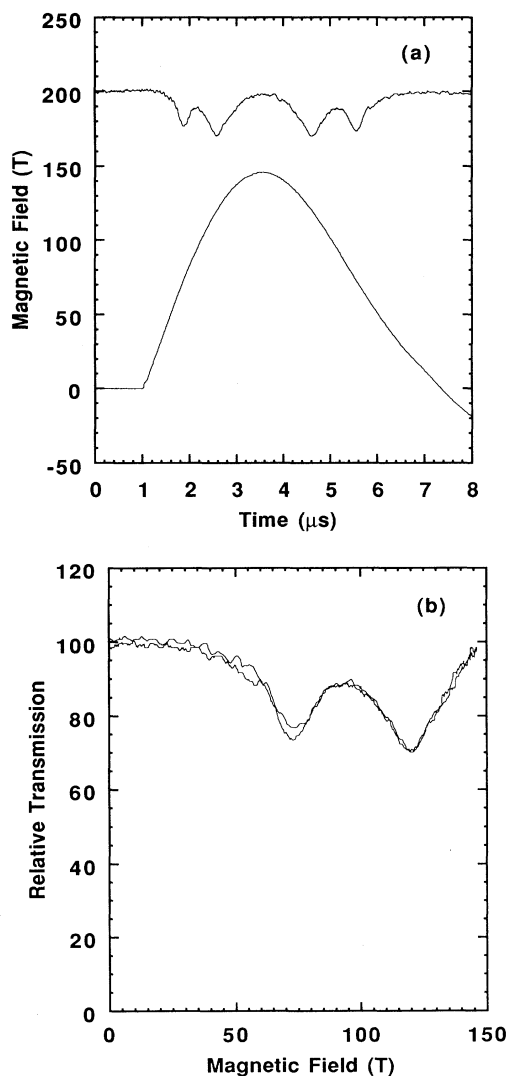


FIG. 1. (a) Example of the recorded traces for far-infrared transmission signal and magnetic field as a function of time. (b) The transmission signal as a function of the magnetic field. Two traces correspond to the trace obtained in the rising slope of the field pulse and the trace in the falling slope, respectively.

TABLE I. The characteristics of the samples studied in the present work.

No.	Type	Thickness (μm)	Carrier density (RT) (cm^{-3})	Carrier mobility (RT) ($\text{cm}^2/\text{V s}$)	Comment
1	<i>n</i>	33.4	3.0×10^{16}	615	
2	<i>n</i>	24.3	3.03×10^{16}	662	
3	<i>n</i>	25.3	2.96×10^{16}	710	no substrate
4	<i>p</i>	13.8	2.6×10^{17}	22	
5	<i>p</i>	14.2	4.2×10^{17}	19	
6	<i>p</i>	14.5	4.8×10^{17}	20	

was less than 3%.²⁵ As radiation sources, we employed pulsed molecular gas lasers,²⁵ a H₂O laser for 16.9, 23, 28, and 119 μm , and a D₂O laser for 36 and 84 μm . An extrinsic photoconductivity of doped Ge was used as a fast detector of the far-infrared radiation at liquid-He temperature. The response time of the detectors including the preamplifier is fast enough to detect a rapid change during the short duration of the resonance.

Figure 1(a) shows an example of the recorded traces of the field pulse and the transmitted radiation from the sample, obtained for *n*-type 3C-SiC at a 36- μm wavelength at room temperature. The transmission data are then plotted as functions of magnetic field in Fig. 1(b). Two cyclotron-resonance absorption peaks are clearly observed as transmission minima. Each of the resonance peaks is observed twice in one pulse, both in the rising and falling slopes of the magnetic field. It should be noted that the coincidence of the two traces ensured a sufficiently fast response of the detector system and the accuracy of the measurement.

The experiments were performed on three *n*-type and three *p*-type 3C-SiC samples grown on carbonized Si(100) surfaces by the CVD method, with the magnetic field oriented along the $\langle 100 \rangle$ crystallographic direction. All the measurements were made in Faraday geometry, i.e., $\mathbf{B} \parallel \mathbf{k}$. The details of the epitaxial growth have been described in Ref. 4. The characteristics of the samples studied in the present work are listed in Table I. *n*-type samples were nondoped (unintentionally doped) films, and had carrier density of about $3 \times 10^{16} \text{ cm}^{-3}$, and a carrier mobility of $6\text{--}7 \times 10^2 \text{ cm}^2/\text{V s}$ at room temperature, while *p*-type samples had $2\text{--}5 \times 10^{17} \text{ cm}^{-3}$ and $20 \text{ cm}^2/\text{V s}$ containing aluminum as acceptors. The thickness of the epitaxial films was 14–34 μm . One of the samples, number 3, was a free-standing film without a substrate.

III. ELECTRON CYCLOTRON RESONANCE IN *n*-TYPE 3C-SiC

A. Results

Figure 2 displays absorption spectra as a function of the magnetic field obtained for *n*-type 3C-SiC, over a wide temperature range at a wavelength of 119 μm . Two clear absorption lines are observed with effective masses of $(0.25 \pm 0.01)m_0$ and $(0.41 \pm 0.01)m_0$. These absorption peaks decrease their intensity and simultaneously narrow their linewidths with decreasing temperature.

They disappear at low temperatures below 50 K, probably due to the carrier freeze-out. This indicates that the lines observed are due to cyclotron resonance of free electrons thermally excited from donor states. The effective masses obtained correspond to m_i^* and $(m_i^* m_l^*)^{1/2}$ of the ellipsoidal energy surfaces at the *X*-point conduction-band minima, and the values are in very good agreement with those of Kaplan *et al.*⁸ obtained at lower magnetic fields with lower photon energies (3.15–4.23 meV).

Absorption spectra are shown in Fig. 3 as a function of the magnetic field with various wavelengths of far-infrared radiations. The resonance field positions increase with increasing photon energies. It should be noted that owing to the ultrahigh magnetic fields the two peaks are clearly resolved even at room temperature for wavelengths of 36, 28, and 23 μm . To observe the $(m_i^* m_l^*)^{1/2}$ peak at wavelengths of 28 and 23 μm , a single-turn coil with an inner diameter of 8 mm was used for generating fields up to 175 T. The results are shown in Fig. 4. The $(m_i^* m_l^*)^{1/2}$ peak is observed at 160 T for

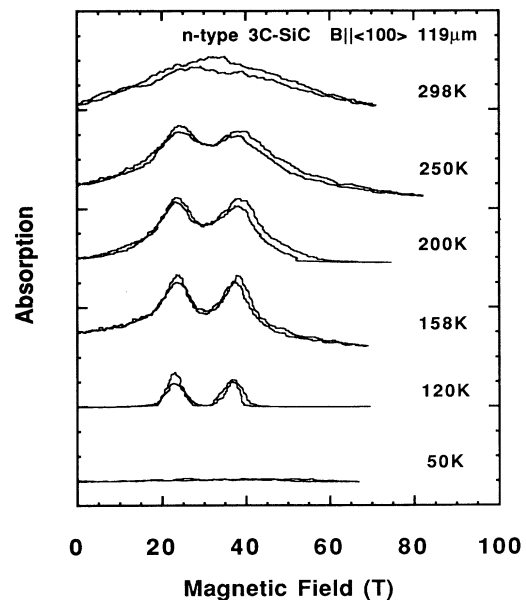


FIG. 2. Absorption spectra as a function of the magnetic field, obtained for *n*-type 3C-SiC at a wavelength of 119 μm over a wide range of temperature 50–298 K. Two clear lines are observed corresponding to m_i^* and $(m_i^* m_l^*)^{1/2}$ of the ellipsoidal energy surface at the *X*-point conduction-band minima.

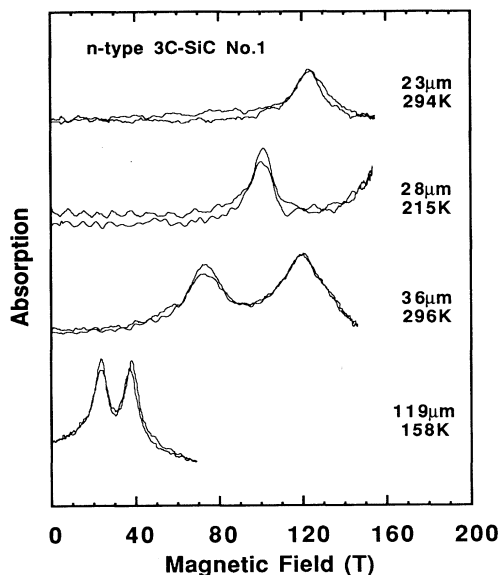


FIG. 3. The wavelength dependence of the cyclotron-resonance trace for *n*-type 3C-SiC. The resonance fields increase with increasing photon energy.

28 μm , but not observed for 23 μm within 175 T. The effective masses at various photon energies are listed in Table II.

In order to exclude the possibility that we might have measured the resonances in the Si substrates, and to check the influence of the interference effects because the thickness of the sample was very close to the wavelength used, three different samples were measured and compared at wavelength of 36 μm . As shown in Fig. 5, the resonance positions are exactly identical for all three samples although they have different line shapes, and this suggests that no peak shifts due to interference effects are included in the data. The data for sample 3, a free-standing film, suggests that peak positions are not influenced by the Si substrate.

B. Discussion on the results of electron CR

The observed cyclotron-resonance transition energy vs resonance magnetic field is plotted in Fig. 6, where two solid lines denote a parabolic band with effective masses of $0.247m_0$ and $0.406m_0$, solid circles denote the present data, and open circles denote the data of Kaplan *et al.*⁸ The slight deviation from the straight lines indicates the

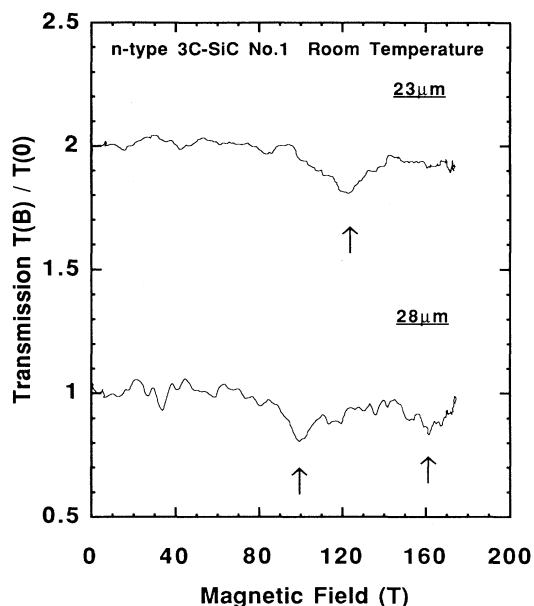


FIG. 4. The cyclotron-resonance traces for *n*-type 3C-SiC at room temperature in magnetic fields up to 175 T at 28- and 23- μm wavelengths.

nonparabolicity of the band. It is obvious from the figure that the conduction band in 3C-SiC is almost parabolic up to the very high-energy range, as expected from the fact that 3C-SiC has a large band gap. Moreover, if the conduction-band edge near the *X* point has a camel's-back structure, anomalous nonparabolicity or photon energy dependence should be observed for the $(m_i^* m_i^*)^{1/2}$ cyclotron-resonance peak. The camel's-back structure is a general feature for zinc-blende-type semiconductors with conduction-band minima at around the *X* point in the Brillouin zone. From Fig. 6, it can be seen that this is not the case for 3C-SiC, and we can conclude that the conduction-band minima in 3C-SiC are located just at the zone boundaries at the *X* point. Otherwise the depth of the camel's-back valley should be much larger than 54 meV.

It is well known that 3C-SiC is a highly polar semiconductor with the Fröhlich coupling constant $\alpha=0.31$,²¹ so that the polaron effect should be taken into account when we analyze the data. From Fig. 6, however, it can be seen that the LO-phonon (at the Γ point) energy, which is 98.7 meV,⁷ is sufficiently higher than the energy range where the present experiments were performed that no

TABLE II. The effective masses of the conduction band in 3C-SiC obtained by cyclotron resonance at various photon energies.

Photon energy (meV)	m_i^*	$(m_i^* m_i^*)^{1/2}$	m_i^*	Reference
53.8	$0.27m_0$			Present work
44.2	$0.26m_0$	$0.42m_0$	$0.68m_0$	Present work
34.4	$0.25m_0$	$0.41m_0$	$0.67m_0$	Present work
10.4	$0.25m_0$	$0.41m_0$	$0.67m_0$	Present work
4.23	$0.247m_0$			Kaplan <i>et al.</i> (Ref. 8)
3.15	$0.247m_0$	$0.406m_0$	$0.667m_0$	Kaplan <i>et al.</i> (Ref. 8)

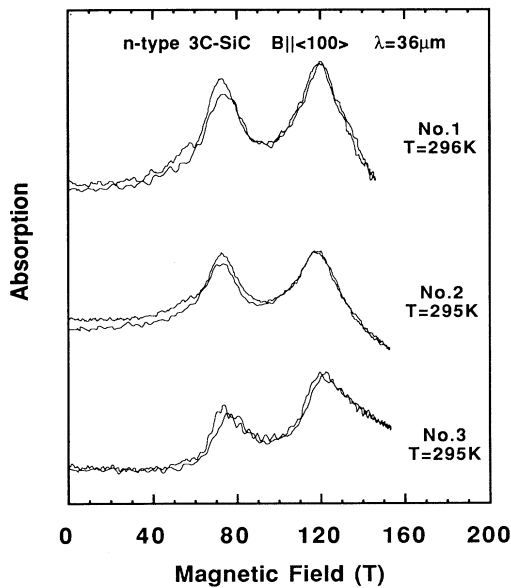


FIG. 5. The sample dependence of the absorption spectrum at 36- μm wavelength. The resonance positions are exactly the same for all three samples, although the line shapes are different. The sample labeled 3 is a free-standing film having no substrate.

significant evidence for the resonance polaron effect is observed. In order to study the electron-LO-phonon interaction, some attempts with CO_2 -laser radiations were also made. None of the experiments with 10.6- μm (117 meV) radiation was successful because of the poor

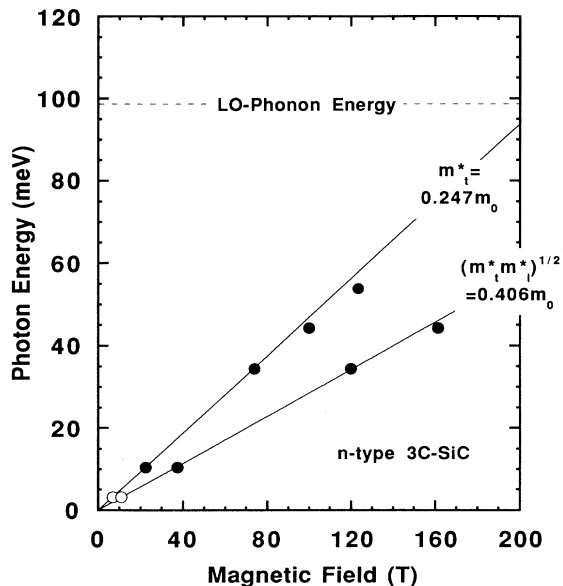


FIG. 6. Observed transition energy vs resonance magnetic field. Two straight lines indicate parabolic bands with effective masses of $0.247m_0$ and $0.406m_0$, respectively. Solid circles denote the present results, and open circles denote the data of Kaplan *et al.* (Ref. 8). Also indicated is the LO-phonon energy at 98.7 meV (Ref. 7) as a dashed line.

transmission, and this must be due to the reststrahlen reflection. Impurity transition studies of the electron-LO-phonon interaction with photon energies above the reststrahlen region are in progress.

We next look into the temperature dependence of the cyclotron resonance linewidth to see if it exhibits the $T^{-3/2}$ behavior expected for acoustic-phonon scattering. This has been also confirmed in the cyclotron-resonance experiments of Kaplan *et al.*⁸ in the low-temperature range 40–100 K. The transverse carrier mobility μ_t estimated from the linewidth of the m_t^* peak at 119- μm wavelength is plotted as a function of temperature T in Fig. 7. As shown in the figure, it obeys the $T^{-3/2}$ law in a wide temperature range 100–300 K. By fitting, it was shown that the curve is very well represented by $\mu_t = 4.8 \times 10^6 T^{-3/2} \text{ cm}^2/\text{Vs}$. Using the same procedure as Kaplan,⁸ we obtained the deformation potential $\Xi = 24 \text{ eV}$, about 10% larger than the value of Kaplan.

As stated in Sec. I, the origin of the residual carriers and the value of the donor ionization energy in 3C-SiC have been the subjects of controversy. Next we consider the temperature dependence of the absorption intensity of the cyclotron resonance in order to obtain a donor ionization energy. Figure 8 shows a logarithmic plot of the cyclotron-resonance absorption intensity as a function of $1/T$. By fitting the function $\exp(-E_d/2kT)$ to the data, we obtain the donor ionization energy $E_d = 19 \text{ meV}$. Yamanaka *et al.* obtained $E_d = 18 \text{ meV}$ for nearly the same samples from the temperature dependence of the Hall coefficient.⁴ Thus the cyclotron-resonance peaks observed are evidently due to the free electrons thermally excited from the donor state having this ionization energy. However, this value is distinct from the value of Kaplan *et al.*,⁸ which is 38 meV, obtained by essentially the same method. In order to obtain detailed information on the energy levels in donor states and to explain the origin of the discrepancy, we studied the impurity transitions as presented in Sec. IV.

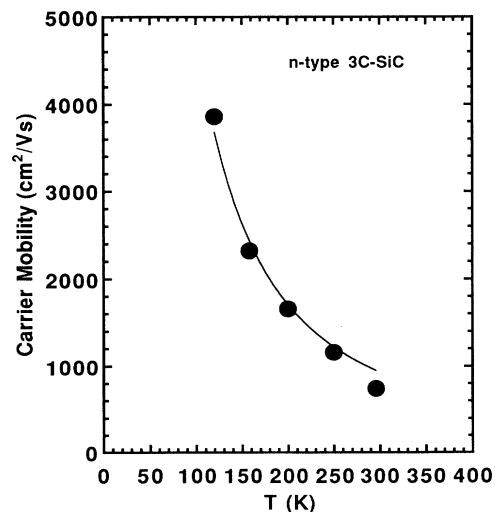


FIG. 7. Temperature dependence of the carrier mobility μ_t , obtained from the cyclotron-resonance linewidth. Solid curve is a fitting curve representing the $T^{-3/2}$ dependence. Data obtained at 119 μm .

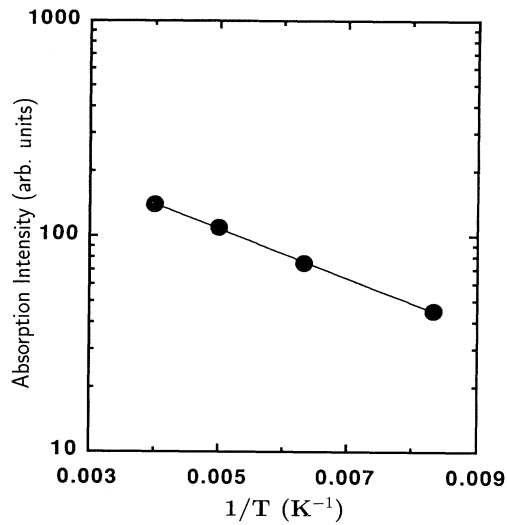


FIG. 8. Temperature dependence of the integrated cyclotron-resonance absorption intensity. The slope of the solid straight line gives a donor ionization energy of 19 meV.

IV. IMPURITY TRANSITIONS IN *n*-TYPE 3C-SiC

Figure 9 shows absorption spectra of *n*-type 3C-SiC obtained at a wavelength of 36 μm , over a wide range of temperature. In addition to two cyclotron-resonance peaks observed only above 98 K, a number of extra peaks are observed at low temperatures. These absorption peaks increase in intensity with decreasing temperature, which suggests that these are the impurity transitions,

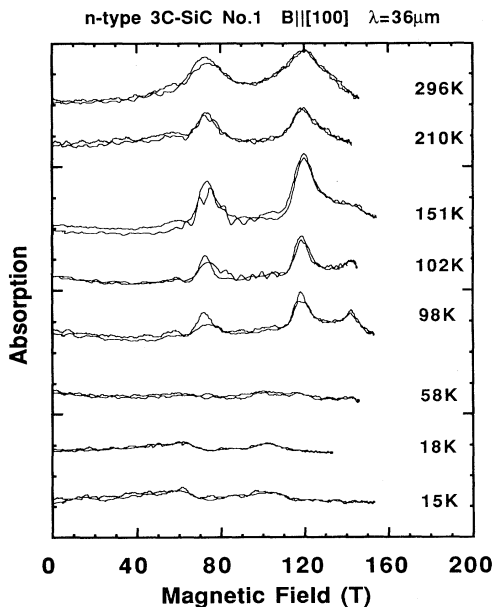


FIG. 9. Magneto-optical absorption spectra of *n*-type 3C-SiC obtained at a wavelength of 36 μm , over a wide range of temperature. In addition to two cyclotron-resonance peaks at 73 and 120 T, which are observed only above 98 K, a number of impurity transitions are observed at low temperatures.

i.e., the transitions involving energy levels in donors. These impurity transitions were also observed at 28-, 23-, and 17- μm wavelengths, but not observed at 119 μm . Some typical spectra are shown in Fig. 10. Figure 11 displays the magnetic-field dependence of the photon energies of transmission minima.

It seems from Fig. 11 that five different kinds of transitions are observed. Five straight lines are drawn in the figure as a guide to the eyes to connect the peaks which are thought of as the same transition. The lowest two lines intersect each other just at zero field with a transition energy of 15 meV, and the highest two lines at 40 meV, while the middle line crosses the zero field at 26 meV. By comparing Fig. 11 with Fig. 6, it is found that the slopes of the lowest two lines in Fig. 11 are similar to the slopes of the two straight lines in Fig. 6 representing cyclotron resonances. This fact enables us to assign the two resonance peaks to the “impurity shifted” cyclotron resonance, i.e., a $1s \rightarrow 2p^+$ [or (000) \rightarrow (110) in the high-field notation] transition for each of the two valleys. According to the well-known equation $E_n = -Ry^*/n^2$ for the energy levels in a shallow hydrogenlike donor, with the experimentally determined relation $E_2 - E_1 = 3 Ry^*/4 = 15$ meV, a value of donor ionization energy 20 meV is obtained. This is consistent with the cyclotron-resonance results.

In many-valley semiconductors such as Ge, Si, and 3C-SiC, the ground state $1s$ [or (000)] is largely influenced by the short-range character of the localized impurity potential in addition to the usual central-cell correction. In other words, nondiagonal matrix elements of the potential between wave functions representing different valleys split the ground state into singlet and triplet levels at zero field. This is one possible explanation for the other lines

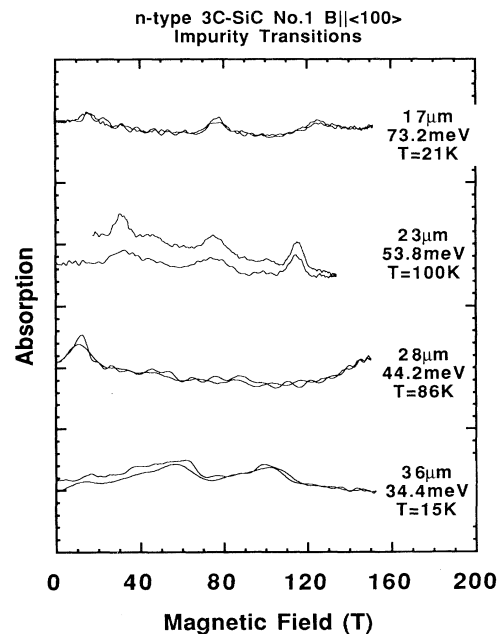


FIG. 10. Impurity transitions observed for *n*-type 3C-SiC at various wavelengths.

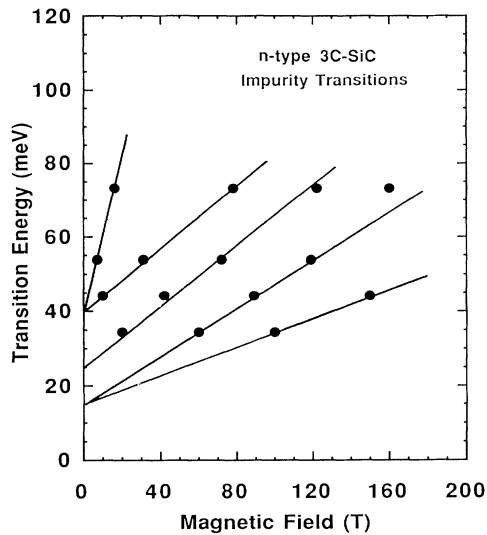


FIG. 11. Impurity transition energy vs magnetic field.

at higher energies. The absorption lines increased their intensity with lowering temperature, but some of them have temperature dependence, which indicates that there is a structure in the ground state. Using the values 26 and 40 meV, it is difficult to consistently interpret these transitions as from the ground state to higher excited levels. Another possibility is that there are three different kinds of donors existing, having binding energies of 19, 35, and 53 meV, respectively. This seems the most plausible explanation when we consider the scatter in the ionization energies reported in the literature. That is, our samples have three different donors with different ionization energies, one of which is the most dominant in electric conduction with an activation energy of 19 meV. One of the three binding energies, say 35 meV, may correspond to the one observed by Kaplan *et al.*⁸

V. HOLE CYCLOTRON RESONANCE IN *p*-TYPE 3C-SiC

Transmission spectra as a function of the magnetic field obtained for *p*-type 3C-SiC at a wavelength of 119 μm over a wide range of temperatures are shown in Fig. 12. At about 210 K, a broad but prominent peak is observed as a transmission minimum with an effective mass of $0.45 m_0$. At other temperatures, however, the peak position shifts towards the lower field and the peak width becomes even broader or disappears. This is probably due to the much lower mobility as well as higher carrier concentration compared with *n*-type samples. The resonance peak which gives $0.45 m_0$ is considered to be due to the light hole of the degenerate valence band, but higher-field measurements are necessary in order to clarify the data. Because of the small spin-orbit splitting Δ [~ 5 meV (Ref. 21)], we can expect a very complicated valence band in a fashion similar to diamond.¹

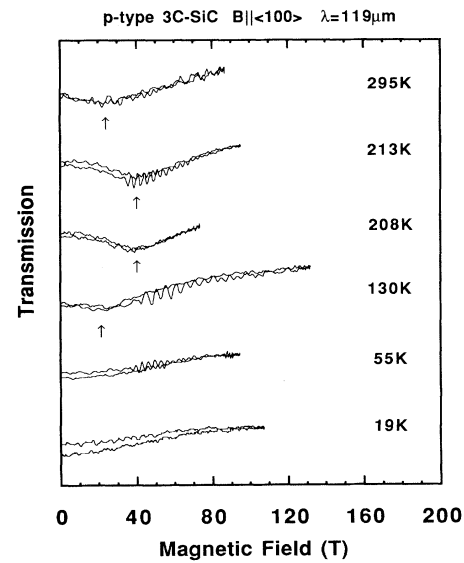


FIG. 12. Transmission spectra for *p*-type 3C-SiC at various temperatures with 119- μm radiations. A broad but prominent cyclotron-resonance peak is observed at around 210 K.

VI. CONCLUSIONS

In *n*-type 3C-SiC, cyclotron resonance was measured in ultrahigh magnetic fields up to 175 T over a wide range of photon energy from 10.4 to 53.8 meV at various temperatures. From the nearly linear photon energy dependence of the cyclotron resonance peak for $(m_i^* m_l^*)^{1/2}$, it was concluded that the conduction-band minima are located at the *X* point without the camel's-back structure. No evidence for the strong electron-LO-phonon coupling was observed in this energy range.

From the temperature dependence of the cyclotron-resonance linewidth, it was confirmed that the dominant carrier scattering mechanism is the acoustic-phonon scattering in a very wide temperature range up to room temperature. The deformation potential of 24 eV was obtained from the coefficient of the $T^{-3/2}$ law. From the temperature dependence of the cyclotron-resonance absorption intensity, the donor binding energy was found to be 19 meV. This value is in agreement with that derived from transport measurements, but in strong disagreement with the value of Kaplan *et al.*⁸

At low temperatures, a number of impurity transitions were observed. Possible assignment was made by considering the magnetic-field dependence of the transition energy, the level degeneracy, and the extrapolated value to zero field, and that the lines observed were from three different kinds of donor states which have different ionization energies: $E_d = 19, 35,$ and 53 meV.

In *p*-type 3C-SiC, a broad but prominent peak was observed at 210 K with an effective mass of $0.45 m_0$. The resonance is possibly due to the light hole in the degenerate valence band, but further investigations and higher mobility samples are necessary in order to clarify the data.

- *Present address: State University of New York at Buffalo, Buffalo, NY 14260.
- †Present address: Himeji Institute of Technology, Harima, Hyogo 678-12, Japan.
- ‡Present address: National Institute of Materials and Chemical Research, Tsukuba, Ibaraki 305, Japan.
- ¹J. Kono, S. Takeyama, T. Takamasu, N. Miura, N. Fujimori, Y. Nishibayashi, T. Nakajima, and K. Tsuji, following paper, *Phys. Rev. B* **48**, 10917 (1993).
- ²SiC exists in three modifications (or polytypes): cubic (*C*), hexagonal (*H*), and rhombohedral (*R*). For the nomenclature in the description of various polytypes, see for example, P. T. B. Shaffer, *Acta Crystallogr. Sec. B* **25**, 477 (1969).
- ³S. Nishino, Y. Hazuki, H. Matsunami, and T. Tanaka, *J. Electrochem. Soc.* **ED-28**, 1235 (1981); S. Nishino, J. A. Powell, and H. A. Will, *Appl. Phys. Lett.* **42**, 460 (1983).
- ⁴M. Yamanaka, H. Daimon, E. Sakuma, S. Misawa, and S. Yoshida, *J. Appl. Phys.* **61**, 599 (1987).
- ⁵M. Shinohara, M. Yamanaka, H. Daimon, E. Sakuma, H. Okumura, S. Misawa, K. Endo, and S. Yoshida, *Jpn. J. Appl. Phys.* **27**, L434 (1988).
- ⁶See for example, L. A. Hemstreet, Jr., and C. Y. Fong, *Phys. Rev. B* **6**, 1464 (1972).
- ⁷P. J. Dean, W. J. Choyke, and L. Patrick, *J. Lumin.* **15**, 299 (1977).
- ⁸R. Kaplan, R. J. Wagner, H. J. Kim, and R. F. Davis, *Solid State Commun.* **55**, 67 (1985).
- ⁹P. Lawaetz, *Solid State Commun.* **16**, 65 (1975).
- ¹⁰N. Miura, G. Kido, M. Suekane, and S. Chikazumi, *J. Phys. Soc. Jpn.* **52**, 2838 (1983).
- ¹¹H. J. van Daal, *Philips Res. Rep. Supp.* **3**, 75 (1965).
- ¹²L. Patrick, *J. Appl. Phys.* **37**, 4911 (1966); **38**, 50 (1967).
- ¹³W. J. Choyke, D. R. Hamilton, and L. Patrick, *Phys. Rev.* **133**, A1163 (1964).
- ¹⁴L. S. Aivazova and Yu. M. Altaiskii, *Fiz. Tekh. Poluprovodn.* **12**, 1452 (1978) [*Sov. Phys. Semicond.* **12**, 861 (1978)].
- ¹⁵K. Sasaki, E. Sakuma, S. Misawa, S. Yoshida, and S. Gonda, *Appl. Phys. Lett.* **49**, 72 (1984).
- ¹⁶A. Suzuki, A. Uemoto, M. Shigeta, K. Furukawa, and S. Nakajima, *Appl. Phys. Lett.* **49**, 450 (1986).
- ¹⁷B. Segall, S. A. Alterovitz, E. J. Haugland, and L. G. Matus, *Appl. Phys. Lett.* **49**, 584 (1986); **50**, 1533 (1987).
- ¹⁸M. Yamanaka, H. Daimon, E. Sakuma, S. Misawa, K. Endo, and S. Yoshida, *Jpn. J. Appl. Phys.* **26**, L533 (1987).
- ¹⁹H. Okumura, M. Shinohara, S. Kuroda, K. Endo, E. Sakuma, S. Misawa, and S. Yoshida, *Jpn. J. Appl. Phys.* **27**, 1712 (1988).
- ²⁰P. Lawaetz, *Phys. Rev. B* **4**, 3460 (1971).
- ²¹D. Bimberg, M. Altarelli, and N. O. Lipari, *Solid State Commun.* **40**, 437 (1981).
- ²²N. Miura, in *Physical Phenomena at High Magnetic Fields*, edited by E. Manousakis, P. Schlottmann, P. Kumar, K. Bedell, and F. M. Mueller (Addison-Wesley, New York, 1992), pp. 589–603.
- ²³S. Takeyama, J. Kono, N. Miura, M. Yamanaka, M. Shinohara, and K. Ikoma, *Physica B* **185**, 384 (1993).
- ²⁴K. Nakao, F. Herlach, T. Goto, S. Takeyama, T. Sakakibara, and N. Miura, *J. Phys. E* **18**, 1018 (1985); S. Takeyama, K. Amaya, T. Nakagawa, M. Ishizuka, K. Nakao, T. Sakakibara, T. Goto, N. Miura, Y. Ajiro, and H. Kikuchi, *ibid.* **21**, 1025 (1988).
- ²⁵G. Kido, N. Miura, K. Kawaguchi, I. Oguro, and S. Chikazumi, *J. Phys. E* **9**, 587 (1976).